Rapid hydraulic collapse as cause of drought-induced mortality in conifers

Matthias Arend[a,1], Roman M. Link[b], Rachel Patthey[a], Günter Hoch[a], Bernhard Schuldt[b], and Ansgar Kahmen[a]

[a]Department of Environmental Sciences, University of Basel, 4056 Basel, Switzerland; and [b]Department of Botany II - Ecophysiology and Vegetation Ecology, Universität Würzburg, 97070 Würzburg, Germany

Edited by Donald R. Ort, University of Illinois at Urbana–Champaign, Urbana, IL, and approved February 19, 2021 (received for review December 21, 2020)

Understanding the vulnerability of trees to drought-induced mortality is key to predicting the fate of forests in a future climate with more frequent and intense droughts, although the underlying mechanisms are difficult to study in adult trees. Here, we explored the dynamic changes of water relations and limits of hydraulic function in dying adults of Norway spruce (*Picea abies* L.) during the progression of the record-breaking 2018 Central European drought. In trees on the trajectory to drought-induced mortality, we observed rapid, nonlinear declines of xylem pressure that commenced at the early onset of xylem cavitation and caused a complete loss of xylem hydraulic conductance within a very short time. We also observed severe depletions of nonstructural carbohydrates, though carbon starvation could be ruled out as the cause of the observed tree death, as both dying and surviving trees showed these metabolic limitations. Our observations provide striking field-based evidence for fast dehydration and hydraulic collapse as the cause of drought-induced mortality in adult Norway spruce. The nonlinear decline of tree water relations suggests that considering the temporal dynamics of dehydration is critical for predicting tree death. The collapse of the hydraulic system within a short time demonstrates that trees can rapidly be pushed out of the zone of hydraulic safety during the progression of a severe drought. In summary, our findings point toward a higher mortality risk for Norway spruce than previously assumed, which is in line with current reports of unprecedented levels of drought-induced mortality in this major European tree species.

trees | drought | hydraulic failure | mortality

Forests are the dominant biomes of the global land area and play, therefore, a crucial role in the global carbon cycle (1, 2). Global observations of forest decline and tree dieback during periods of intense drought have stressed the need to understand and predict the vulnerability of trees to more frequent occurrences of such climate extremes in the future (3, 4). The underlying mechanisms of drought-induced forest decline have remained remarkably difficult to study in adult trees, leaving some uncertainty in projecting the future of Earth's forests. Two interconnected concepts have evolved from past research, explaining the physiological cause of drought-induced tree mortality either by xylem cavitation, loss of xylem hydraulic conductance and lethal tissue dehydration (hydraulic failure), or by disorders of CO_2 fixation and carbon metabolism, leading to a fatal depletion of nonstructural carbohydrates (carbon starvation) (5–7). While these concepts provide the mechanistic basis for the current understanding of tree responses to drought, recent work put particular emphasis on hydraulic failure as the cause of drought-induced tree mortality across multiple tree taxa (8–10).

Direct physiological evidence for the hydraulic vulnerability of trees to drought mostly comes from glasshouse and laboratory studies, with saplings or excised tree organs subjected to artificially imposed drought, tissue drying, or centrifugal forces (11–13). These studies revealed potential thresholds for lethal hydraulic failure, which enabled the employment of species-specific hydraulic safety margins, describing a safe operating range of xylem pressure under drought (14–17). As mechanistically derived functional traits, hydraulic safety margins are thought to describe for a given species the degree of conservatism in the control of plant water relations and thus are strongly associated with species-specific drought tolerances (8, 9, 15). On the individual tree level, however, a tree's probability of dying from drought at a given point in time depends on the individual's health and water status as well as its biotic and abiotic environment, which hydraulic traits alone cannot predict. For that reason, recent work on tree drought responses has expanded its focus from merely quantifying empirical thresholds for hydraulic failure and associated safety margins toward predicting the time it takes to reach them (18–22).

In conifers, thresholds for lethal hydraulic failure have been suggested to correspond to the xylem pressure at which 50% loss of hydraulic conductance (P_{50}) occurs (11, 23, 24), though a recent study indicates that potted pine seedlings may even recover from more severe losses of hydraulic conductance (13). Other definitions, accounting for close coordination of stomatal regulation and xylem hydraulic function, consider a higher xylem pressure at which 12% hydraulic conductance is lost (P_{12}) as a more conservative threshold of hydraulic function (18). Regardless of different reference threshold values, direct evidence of widespread hydraulic failure in adult, field-grown conifers is exceedingly rare, as are studies that document hydraulic failure under a naturally occurring drought (25, 26). We therefore do not only lack evidence of hydraulic failure as the proximate cause of drought-induced tree mortality in the field but also empirical support for conceptual or mechanistic models predicting the mortality of

Significance

Sound knowledge of the limits of tree hydraulic function is crucial to understand drought-induced tree mortality, although the mechanisms are difficult to study in adult trees. We explored the dynamic changes that the tree hydraulic system undergoes during the progression of a severe drought in dying adults of Norway spruce. Xylem pressure and hydraulic conductance showed sudden, nonlinear declines that commenced at surprisingly low levels of xylem embolism and caused a rapid collapse of the tree's hydraulic system and tree death. These observations provide striking field-based evidence for hydraulic failure in adult conifers that are on the trajectory to drought-induced mortality. The nonlinear temporal dynamic of dehydration suggests a higher mortality risk than previously assumed for this major European tree species.

Author contributions: M.A. and A.K. designed research; M.A., R.M.L., R.P., G.H., and A.K. performed research; M.A. and R.M.L. analyzed data; and M.A., R.M.L., G.H., B.S., and A.K. wrote the paper.

The authors declare no competing interest.

This article is a PNAS Direct Submission.

[1]To whom correspondence may be addressed. Email: matthias.arend@unibas.ch.

This article contains supporting information online at https://www.pnas.org/lookup/suppl/doi:10.1073/pnas.2025251118/-/DCSupplemental.

Published April 12, 2021.

ECOLOGY

adult, field-grown trees, with hydraulic thresholds obtained from saplings in laboratory studies.

Results and Discussion

Here, we took advantage of the exceptional 2018 Central European drought that caused widespread damage to Central European forests (27, 28) and explored the dynamic changes of tree water relations and hydraulic function in tall, adult individuals of Norway spruce (*Picea abies* L.) that died during this event. These unique observations allowed us to investigate the limits of tree hydraulic function on the edge to drought-induced mortality and test theoretical considerations in current concepts of drought-induced mortality under the conditions of a real-world drought (22). Our field observations during the 2018 vegetation season revealed unusually strong moisture stress on tree water relations as a result of low and irregular summer precipitation and high atmospheric water demand (Fig. 1*A*). Volumetric soil water content decreased on average from 0.39 $m^3 \cdot m^{-3}$ in June to values below 0.12 $m^3 \cdot m^{-3}$ in early August and remained at this very low level until the end of the vegetation season in late October. The moisture stress was aggravated by strongly elevated vapor pressure deficits (vpd), reaching exceptionally high daytime averages (0600 to 1800 Central European Time [CET]) of up to 2.65 kPa in late July and early August.

The resulting drought led to a linear decline of midday xylem pressure (P_{md}) from values between −1.4 and −1.6 MPa in late spring and early summer to between −2.3 and −2.8 MPa in late summer and early autumn (excluding dying trees, Fig. 1*B*). The observed P_{md} values thus reached lower levels than the previously reported minimum value of −2.2 MPa for adult, drought-stressed individuals of Norway spruce growing in a different forest stand in the same region (29). After drought release in autumn, water relations of surviving trees recovered quickly, with P_{md} reaching −0.9 MPa toward the end of the year. Importantly, not all trees followed the trend of a linearly declining P_{md}. During the drought, some trees showed a rapid, nonlinear decline of P_{md} to exceptionally low values, which was followed by canopy dieback and ultimately tree death in all these trees (5 of 12 studied trees, Fig. 1*C*). The lowest xylem pressures observed in the dying trees were close to or even exceeded the detection limit of −7.0 MPa before dieback of the canopy occurred.

Theory predicts that a xylem pressure falling to very low values must have serious consequences for the tree's hydraulic integrity. This is exemplified by xylem vulnerability curves that indicate a nonlinear decrease of hydraulic conductance, with declining xylem pressure due to xylem embolism formation. Vulnerability curves that we established for branches of a subset of the studied Norway spruce trees revealed a P_{12} threshold for the onset of excessive cavitation and embolism spread at an average xylem pressure of −3.1 MPa and a P_{50} threshold for lethal hydraulic failure at an average xylem pressure of −3.6 MPa (Fig. 2*A* and *SI Appendix*, Table S2). Stomatal closure occurred at −2.1 MPa (P_{st}) (*SI Appendix*, Fig. S2). Our field observations showed that surviving trees maintained P_{md} mostly above P_{12} and always far above P_{50}, while dying trees did not (Fig. 1*B*). This implies that dying trees must have experienced massive loss of hydraulic conductance. We validated this prediction by assessing the degree of native xylem embolism in the canopy of the investigated trees. We found that dying trees had their xylem completely embolized with a percent loss of conductance (PLC) of 100%, while surviving trees had their hydraulic system generally intact with PLC largely <12% (Fig. 2*B*). Notably, PLC values in the medium range of xylem hydraulic conductance (20 to 99%) were hardly observed in situ, suggesting that the tree hydraulic system collapsed in a very short time. These findings give strong evidence that drought-induced mortality in adult conifers is associated with a complete failure of xylem water transport and illustrate that this failure can occur very rapidly. The sudden

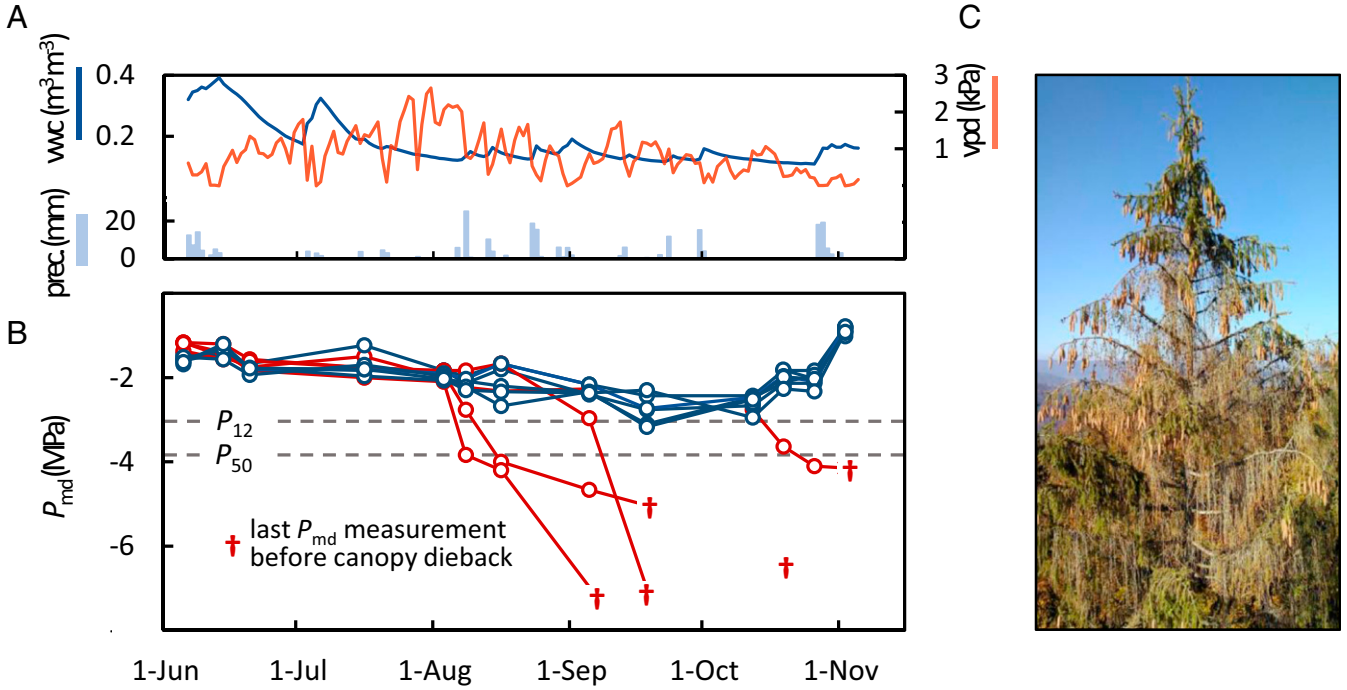

Fig. 1. Sudden collapse of water relations in dying spruce trees during the 2018 drought event. (*A*) Low/irregular precipitation (prec.), elevated daytime vpd, and low soil water content (vwc) led to an exceptionally severe drought in summer and autumn 2018. (*B*) Gradual decline of P_{md} throughout the 2018 drought and recovery toward the end of the year (lines/open circles show individual trees). Some trees show a sudden, nonlinear decline of P_{md} and subsequent canopy dieback (red lines/symbols). Dashed lines indicate P_{12} and P_{50} thresholds to cavitation derived from ex situ vulnerability curves (cf Fig. 2*A* and *SI Appendix*, Table S2). (*C*) Spruce tree with early symptoms of canopy dieback at the last date of P_{md} measurement.

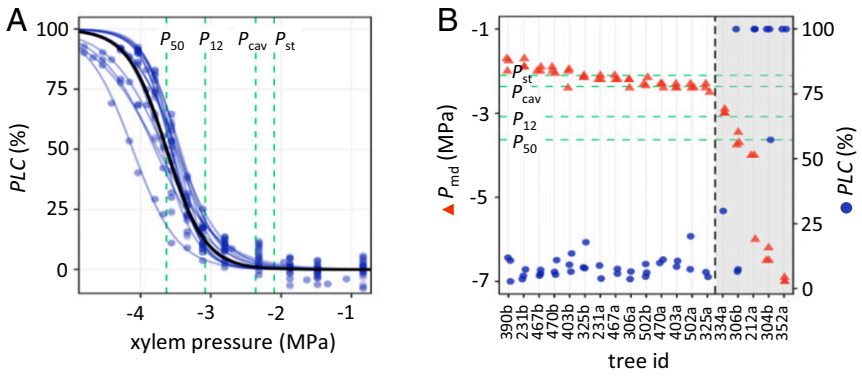

Fig. 2. Vulnerability curves and field observations of xylem pressure and hydraulic conductance reveal the limits of hydraulic function. (*A*) Laboratory-derived vulnerability curves. PLC versus xylem pressure (blue: individual trees and black: population-level predictions, cf *SI Appendix*, Table S2). A safe range of xylem pressures is defined by the point of P_{st} and the xylem pressure at the P_{cav}, which may be even less negative than the xylem pressure at P_{12} (−3.08 MPa) and was arbitrarily placed in the range between P_{st} and P_{12}. With more negative pressures, the mortality risk rises until reaching a xylem pressure at P_{50} (−3.63 MPa). (*B*) Comparison of P_{md} and the naturally occurring loss of xylem hydraulic conductance, PLC. Data were collected at two sampling days during the 2018 drought. Dying trees (gray area) show $P_{md} < P_{cav}$ and high PLC. Red and blue symbols show concomitant measurements of P_{md} and PLC, respectively, on single trees, (cf *SI Appendix*, Table S3).

hydraulic failure is most likely the consequence of the pronounced drop in xylem pressure. Notwithstanding the low number of observations in the intermediate PLC range, our data provide an important validation of a laboratory-derived xylem vulnerability curve with in situ observations of hydraulic failure in trees (*SI Appendix*, Fig. S1 and Tables S2 and S3).

To further test if the observed trees actually died from a sudden collapse of their hydraulic system, we investigated other potential causes of tree mortality. The occurrence of biotic mortality factors (bark beetle infestation and fungal infection) could be excluded after inspection of stems felled after tree death. On the other hand, all surviving and dying tree individuals showed clear signs of a disturbed carbon metabolism during the 2018 drought event. We found strongly impaired rates of photosynthesis and unusually low concentrations of nonstructural carbohydrates (sugars and starch) in needles, bark, and branch wood tissue during the 2018 drought event (*SI Appendix*, Table S1 and Fig. 3). Tissue concentrations of starch reached lower levels than previously reported for drought-exposed Norway spruce trees (29–31), though comparison to other studies might be biased by the usage of different laboratory protocols (32). Nonetheless, our results point to a severe depletion of carbohydrate reserves. Most importantly, low tissue concentrations of nonstructural carbohydrates, with basically no detectable starch, occurred during peak drought in dying as well as surviving trees. The latter, however, showed a fast increase in starch after drought weakening in autumn and recovery in the following year. Our data therefore indicate that adult conifer trees may survive a drought-induced depletion of their carbohydrate reserves, and that carbon starvation is unlikely to be the proximate cause of the mortality we report here.

Our observations shed important light on the temporal dynamics of dehydration and hydraulic failure in dying trees under the conditions of a real-world drought. Most notably, the decline of xylem pressure leading to hydraulic failure shows a fast, nonlinear progression with time, in that P_{md} first declines at a slow rate but then suddenly drops to much lower values as the drought continues. Typically, such nonlinear dynamics involve specific tipping points, in which strong changes in the state of a system occur (33). A tipping point, in which a tree starts losing control over its hydraulic system, may occur after P_{st}, when extractable water reserves in drying soils run out and continuing residual water loss can no longer be compensated by water uptake from the soil or the tree's internal water storage (19, 34–36). Indeed, modeling approaches and experimental work emphasize the significance of the soil–root hydraulic continuum and root hydraulic conductance for the control of plant water relations under the conditions of increasing drought (37–39). Given the steep increase of water tension that typically arises in drying soils, water absorption through roots will decline in a nonlinear fashion, and water diffusion to the xylem can be further constrained by low root hydraulic conductance. In the following, the tree will enter a critical hydraulic stage in which even small residual water losses lead to a rapid decline in xylem pressure. In line with this assumption, a model of tree mortality under extreme drought suggests that temperature-dependent changes in cuticular permeability and high leaf-to-air vpd may cause sudden increases in residual water loss resulting in rapid hydraulic failure (40). These processes may be exacerbated by interactions with tree carbohydrate status, which can directly affect the hydraulic state of a tree via its role in osmotic regulation (6, 41).

A further potential mechanism for a rapid drop in xylem pressure refers to the so-called "runaway cavitation" phenomenon, in which self-enhancing cavitation lowers hydraulic conductance and xylem pressure in a vicious circle (42). However, mechanistic modeling suggests that this process is unlikely to play a substantial role before reaching very high levels of embolism due to the buffering effect of the water liberated from embolized conduits (43). In addition, it is unlikely that embolism formation is driving the decline in water potential for the simple reason that embolism occurs under conditions when conductivity is not limiting water transport to the canopy because stomata are closed and transpiration demand is low (36). Regardless of the actual mechanism, the tree hydraulic system that delivers water from the soil to the canopy will undergo rapid changes. Such a temporally nonlinear behavior of tree water relations under severe drought has also been observed in other tree species (20, 44) and might therefore be considered a general—but mostly overlooked—phenomenon.

The notion of strong nonlinearity in the function of a tree's hydraulic system during the progression of a severe drought may have important implications for characterizing the vulnerability of trees to drought-induced mortality. This is in particular true if the mortality risk of a tree under drought is described as the time that remains before crossing a specific threshold to lethal hydraulic failure (21). In conifers, this threshold has been suggested to be the xylem pressure at which P_{50} occurs. Our field observation of adult trees shows, however, that processes leading to a rapid deterioration of tree water status and tree death set in long

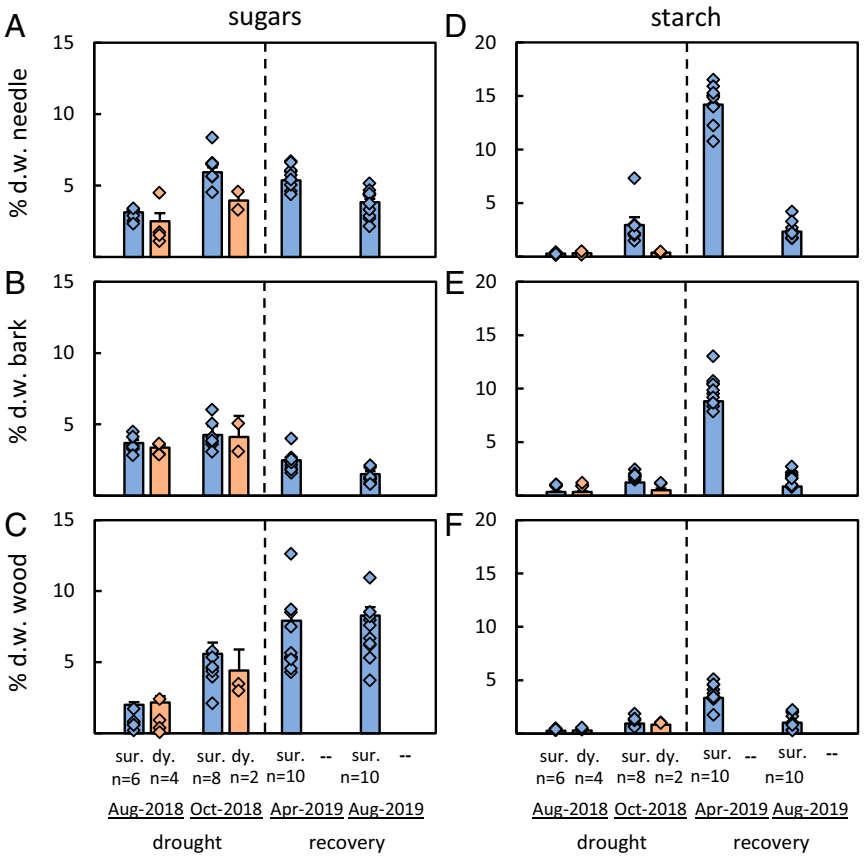

Fig. 3. Drought-induced depletion of nonstructural carbohydrates in dying and surviving trees. Concentrations of sugars (*A*–*C*) and starch (*D*–*F*) in needles, bark, and branch wood during the 2018 drought and after drought weakening in autumn and recovery in 2019. Needles and particularly wood of surviving and dying trees show low concentrations of sugars during the 2018 drought compared to the 2019 season. Starch is completely depleted in all tissues during the peak of the drought in August 2018 (mean ± SE). Diamonds show the measurements in single trees (sur. = surviving trees and dy. = dying trees). d.w., dry weight.

before P_{50} is reached (11, 23, 24) and may even be triggered in a nonlinear fashion above the traditional "air-entry" threshold of P_{12} (14, 45). It suggests that the commonly used threshold values of xylem pressure are not useful under field conditions, and that the vulnerability of Norway spruce to hydraulic failure and mortality is more accurately characterized by less negative xylem pressure thresholds than previously thought.

Based on the above considerations, we summarize our observations on dying Norway spruce trees in a conceptual framework that describes the temporal trajectory to hydraulic failure in these trees and their actual vulnerability to drought-induced mortality at a given point in time (Fig. 4). It shows a mostly linear decline of xylem pressure and decay of hydraulic safety after P_{st} that is likely driven by cuticular and residual stomatal conductance. Once a tree is pushed over a tipping point of incipient embolism formation, it enters a zone of nonlinearly increasing mortality risk, where the probability of hydraulic recovery decreases rapidly until the lethal level of hydraulic failure at P_{50} is reached. In Norway spruce, this tipping point is reached at a xylem pressure of about −2.4 MPa, in which the early onset of xylem cavitation and the first loss of xylem hydraulic conductance occur (Fig. 2 *A* and *B*). We refer to this point as P_{cav} (cav = early onset of cavitation), following a previous plant hydraulic concept (17). From P_{cav} onwards, xylem pressure and hydraulic conductance drop so rapidly that the chance for the tree to recover is very low. Using P_{cav} instead of P_{50} to describe the vulnerability of trees in a progressing drought implies that Norway spruce trees may face higher risks of drought-induced mortality than previously thought. If, for example, our observation of P_{st} in Norway spruce at a xylem pressure of −2.1 MPa (*SI Appendix*, Fig. S2) is related to the xylem pressure at P_{cav}, a remaining hydraulic safety of only 0.3 MPa becomes evident. It thus challenges the previous report of a large safety margin of 1.7 MPa between observed minimum xylem pressure and P_{50} in Norway spruce, which naturally lead to the wrong assumption of a low mortality risk in this species (29).

Our study provides a first comprehensive report on the temporal dynamics of hydraulic collapse in adult conifers that are on the trajectory to drought-induced mortality. We show, under the conditions of a severe real-world drought, that nonlinear progression of dehydration can lead to a catastrophic collapse of tree water relations and ultimately tree death. This nonlinear dynamic of dehydration may trigger hydraulic failure before commonly assumed thresholds for hydraulic failure at P_{12} or P_{50} have been reached. It also underpins the importance of recent modeling approaches to mortality, focusing on the time that a tree can withstand in a progressing drought after P_{st} (18, 22). This time has been suggested to be a key adaptive trait for predictions of drought-induced mortality across multiple tree taxa and growth forms (21, 34, 35, 46). In line with current assumptions (18), our data show that this time needs to be defined with more conservative thresholds than previously thought in order to realistically predict the vulnerability of Norway spruce to drought-induced mortality.

Materials and Methods

Research Site. All measurements were conducted on the Swiss Canopy Crane II site in Hölstein/BL, Switzerland (47°26′17″N, 7°46′37″E; 550 m above sea

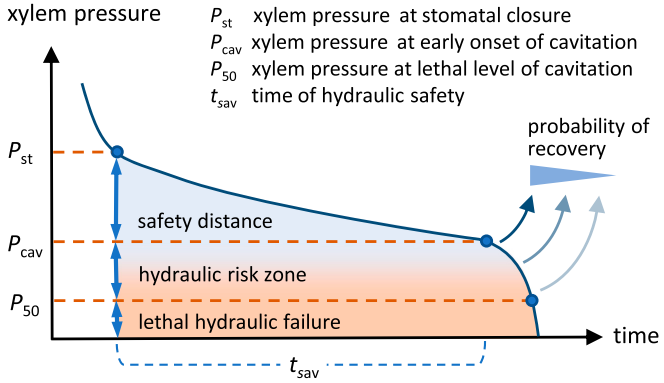

Fig. 4. Trajectories of tree water relations and the limits of hydraulic function during the progression of a mortality-inducing drought. At the beginning of a drought, an initial drop of xylem pressure provokes P_{st}. As the drought continues, xylem pressure declines gradually, leading to a mostly linear decay of the hydraulic safety distance until the xylem pressure at the P_{cav} is reached. Beyond this point, the tree enters a hydraulic risk zone, in which the xylem pressure declines nonlinearly, and the probability of hydraulic recovery decreases rapidly. The tree hydraulic system collapses irreversibly if the xylem pressure drops below P_{50}, in which lethal levels of cavitation occur. The time period between P_{st} and P_{cav} describes the time of relative hydraulic safety, t_{sav}.

level). The research site is situated in the Swiss Jura mountains, in a mixed temperate forest, on calcareous loamy soil. The average regional climate conditions are 9 °C annual temperature and 1,009 mm annual precipitation (SwissMeteo station Basel-Binningen). The technical infrastructure comprises 20 automated soil moisture probes (5TM, Decagon Inc.) positioned at 10 cm depth across the site; a fully equipped weather station, installed 2 m above ground (Davis Vantage Pro2, Davis Instruments Corporation); and a canopy crane with a height of 45 m and a crane radius of 50 m. The forest vegetation of the research site is dominated by European beech (*Fagus sylvatica* L.) and Norway spruce (*P. abies* L.) of different age and size classes and includes nine admixed tree species. During the course of the exceptionally severe 2018 drought, 10 tall, adult Norway spruce trees died, representing a relative loss of basal area of 15.1% for this tree species.

Characterization of the 2018 Drought. Meteorological data collected from three long-running SwissMeteo stations of the Federal Office of Meteorology and Climatology (Basel-Binningen 47°54′11″, 7°58′35″, Zürich-Fluntern 47°37′79″, 8°56′57″, Bern-Zollikofen 46°99″07″, 7°46′41″), located in different directions and distances around the study site, were used to evaluate how the regional weather conditions in summer and early autumn 2018 (June to October) diverged from the respective long-term trend (1864 to 2018). Across the three stations, the average daily temperature was increased by 3 °C, the average atmospheric vapor pressure deficit was increased by 54%, and the average precipitation sum was reduced by 44.4% (*SI Appendix*, Fig. S3 *A* and *B*). These changes resulted in an exceptionally severe drought in 2018 as indicated by the Standardized Precipitation Evaporation Index. It showed that the region around the study site experienced the second-most severe summer drought since starting the instrumental record of climate data in Switzerland in 1864 [*SI Appendix*, Fig. S3*C* (47)].

Study Trees. In late spring 2018, before the onset of the summer drought, 10 healthy, adult individuals of Norway spruce with a height of ~35 m and age of >100 y were randomly selected within the crane radius area for assessing seasonal fluctuations of canopy xylem pressure (P_{md}). Trees which died in the course of the unexpected summer and autumn drought were replaced by other randomly selected trees to keep the sample size at $n = 10$. Analyses of the native loss of xylem hydraulic conductance (*PLC*), xylem hydraulic vulnerability, gas exchange, and nonstructural carbohydrates were conducted on the same trees used for regular P_{md} measurements.

Measurement of Xylem Pressure. P_{md} was measured with a Scholander's type pressure chamber (PMS Instrument Company) on three excised twigs per tree, collected between 1200 and 1400 CET with the crane in the upper canopy of 10 trees. The measurements were conducted from June to November 2018, in regular intervals of about 2 wk.

Measurement of Native Xylem Hydraulic Conductance. A total of 46 branch samples of ~100 cm length were collected with the crane in the upper canopy of the same spruce trees used throughout the 2018 season for P_{md} measurements. Two sampling campaigns were conducted in early September and mid October 2018, on days when P_{md} values were measured. Samples were immediately stored in dark humidified plastic bags and transported to the laboratory at the University of Basel, where conductance was measured with an Xyl'Em-Plus embolism meter (Bronkhorst France). Prior to the measurement, samples were recut under water at least twice while letting the xylem tension relax for 20 min to avoid excision artifacts. Stem segments of on average 47 mm length and 6.9 mm diameter were excised at least 15 cm upstream of the original cut, debarked, and their cut surfaces cleaned with a razor blade. Conductance measurements were performed submerged in water using a pressure head of ~4 kPa, and a measurement solution of 10 mM KCl and 1 mM $CaCl_2$ in degassed demineralized water filtered to a particle size of 0.2 μm. The hydraulic conductance of the samples was measured before (K_i) and after (K_f) rehydrating the samples for at least 48 h in measurement solution under vacuum. The PLC (%) was then calculated as PLC = 100 (1—K_i/K_f) based on readings from the XylWin 3.0 software (Bronkhorst France).

Construction of Xylem Vulnerability Curves. The flow-centrifuge technique was used to construct xylem vulnerability curves. A total of 14 branch samples were collected in January 2019 with the crane in the upper canopy from 7 of the 10 trees used for the last regular P_{md} measurements. The branch samples were transported to the University of Würzburg on the same day, stored at 4 °C, and processed within 10 d. In the laboratory, the samples were recut under water to a length of 27.5 cm, debarked, cleaned at their ends with a sharp razor blade, and placed in a custom-made rotor (S. Delzon). The rotor was then mounted to a modified Sorvall RC-5 C centrifuge (Thermo Fisher Scientific) controlled with the CaviSoft version 5.2 software (University of Bordeaux) to measure the loss of conductivity, with increasingly more negative water potentials. Vulnerability curves for the flow-centrifuge method were fitted in R version 3.6.2 using a nonlinear mixed model with lognormal errors (R package nlme version3.1–144) based on the conductivity-based form of the exponential sigmoid model previously provided (48). The in situ vulnerability curve was fitted with nonlinear least squares (base R function nls) using an analogous model.

Measurement of Photosynthesis. Instant net photosynthesis was measured under dry conditions on a sunny day in September 2018, and for comparison under wet conditions on a sunny day in August 2019, in the upper canopy between 1400 and 1600 CET using a portable photosynthesis system (LI-COR 6400, LI-COR Inc.) equipped with a clear conifer chamber. The conditions inside the chamber were kept constant at 400 ppm CO_2, a flow rate of 500 μmol · s^{-1}, and ambient temperature and humidity. Variable needle mass inside the conifer chamber was corrected by measurements of needle area using a bench-top leaf area meter (LI 3100C- LI-COR Inc.).

Analysis of Nonstructural Carbohydrates. Levels of nonstructural carbohydrates (starch and the low molecular weight carbohydrates glucose, fructose, and sucrose) were measured under dry conditions in August and October 2018 and for comparison under wet conditions in April and August 2019. The enzymatic–photometric method was used as previously described in detail (49). In short, low molecular weight sugars were extracted from plant powder with 80% ethanol at 90 °C. After the splitting of sucrose with invertase and the conversion of fructose to glucose by isomerase, the sum of glucose, fructose, and sucrose (referred to here as "sugars") was determined photometrically at 340 nm after the conversion of glucose to gluconate using hexokinase (glucose assay reagent, Sigma Aldrich). In the remaining pellet, starch was degraded to free glucose by sequentially adding α-amylase and amyloglucosidase. The total amount of free glucose after starch degradation was determined photometrically as described above. A dilution series from a commercial glucose standard solution (1 mg/mL^{-1}) was used to quantify glucose. Sucrose, fructose, and starch solutions, as well as two different plant powders (orchard leaves and cereal grains), were included in each analysis run to ensure correct enzyme activities and reproducibility of the analyses. All chemicals were purchased from Sigma Aldrich. Tissue concentrations in needles, bark, and branch wood were expressed on a dry matter basis.

Data Availability. All data are included in the article and/or *SI Appendix*.

ACKNOWLEDGMENTS. We thank C. Bloch for helping us with the measurements of xylem pressure, S. Förster for technical support in the laboratory, and Lucio Rizzelli for operating the canopy crane. We also thank C. Zahnd for providing statistical support. This study was financially supported by the Swiss Federal Office for the Environment.

1. FAO and UNEP, The State of the World's Forests 2020: Forests, biodiversity and people. https://doi.org/10.4060/ca8642en.
2. Y. Pan *et al*., A large and persistent carbon sink in the world's forests. *Science* **333**, 988–993 (2011).
3. C. D. Allen, D. D. Breshears, N. G. McDowell, On underestimation of global vulnerability to tree mortality and forest die-off from hotter drought in the Anthropocene. *Ecosphere* **6**, 1–55 (2015).
4. IPCC, "Climate change 2014: Synthesis report. Contribution of working groups I, II and III to the fifth assessment report of the intergovernmental panel on climate change" in *IPPC's Fifth Assessment Report*, R. K. Pachauri, L. A. Meyer, Eds. (IPCC, Geneva, Switzerland, 2014), pp. 151.
5. N. McDowell *et al*., Mechanisms of plant survival and mortality during drought: Why do some plants survive while others succumb to drought? *New Phytol.* **178**, 719–739 (2008).
6. N. G. McDowell, Mechanisms linking drought, hydraulics, carbon metabolism, and vegetation mortality. *Plant Physiol.* **155**, 1051–1059 (2011).
7. W. R. L. Anderegg *et al*., The roles of hydraulic and carbon stress in a widespread climate-induced forest die-off. *Proc. Natl. Acad. Sci. U.S.A.* **109**, 233–237 (2012).
8. W. R. L. Anderegg *et al*., Meta-analysis reveals that hydraulic traits explain cross-species patterns of drought-induced tree mortality across the globe. *Proc. Natl. Acad. Sci. U.S.A.* **113**, 5024–5029 (2016).
9. H. D. Adams *et al*., A multi-species synthesis of physiological mechanisms in drought-induced tree mortality. *Nat. Ecol. Evol.* **1**, 1285–1291 (2017).
10. J. S. Powers *et al*., A catastrophic tropical drought kills hydraulically vulnerable tree species. *Glob. Change Biol.* **26**, 3122–3133 (2020).
11. M. Urli *et al*., Xylem embolism threshold for catastrophic hydraulic failure in angiosperm trees. *Tree Physiol.* **33**, 672–683 (2013).
12. S. Li *et al*., Leaf gas exchange performance and the lethal water potential of five European species during drought. *Tree Physiol.* **36**, 179–192 (2016).
13. W. M. Hammond *et al*., Dead or dying? Quantifying the point of no return from hydraulic failure in drought-induced tree mortality. *New Phytol.* **223**, 1834–1843 (2019).
14. F. C. Meinzer, D. M. Johnson, B. Lachenbruch, K. A. McCulloh, D. R. Woodruff, Xylem hydraulic safety margins in woody plants: Coordination of stomatal control of xylem tension with hydraulic capacitance. *Funct. Ecol.* **23**, 922–930 (2009).
15. D. M. Johnson, K. A. McCulloh, D. R. Woodruff, F. C. Meinzer, Hydraulic safety margins and embolism reversal in stems and leaves: Why are conifers and angiosperms so different? *Plant Sci.* **195**, 48–53 (2012).
16. B. Choat *et al*., Global convergence in the vulnerability of forests to drought. *Nature* **491**, 752–755 (2012).
17. S. Delzon, H. Cochard, Recent advances in tree hydraulics highlight the ecological significance of the hydraulic safety margin. *New Phytol.* **203**, 355–358 (2014).
18. N. Martin-StPaul, S. Delzon, H. Cochard, Plant resistance to drought depends on timely stomatal closure. *Ecol. Lett.* **20**, 1437–1447 (2017).
19. C. J. Blackman *et al*., Toward an index of desiccation time to tree mortality under drought. *Plant Cell Environ.* **39**, 2342–2345 (2016).
20. C. J. Blackman *et al*., Drought response strategies and hydraulic traits contribute to mechanistic understanding of plant dry-down to hydraulic failure. *Tree Physiol.* **39**, 910–924 (2019).
21. C. J. Blackman *et al*., Desiccation time during drought is highly predictable across species of Eucalyptus from contrasting climates. *New Phytol.* **224**, 632–643 (2019). Correction in: New Phytol. 229, 1822–1823 (2021).
22. W. M. Hammond, H. D. Adams, Dying on time: Traits influencing the dynamics of tree mortality risk from drought. *Tree Physiol.* **39**, 906–909 (2019).
23. T. J. Brodribb, H. Cochard, Hydraulic failure defines the recovery and point of death in water-stressed conifers. *Plant Physiol.* **149**, 575–584 (2009).
24. T. J. Brodribb, D. J. M. S. Bowman, S. Nichols, S. Delzon, R. Burlett, Xylem function and growth rate interact to determine recovery rates after exposure to extreme water deficit. *New Phytol.* **188**, 533–542 (2010).
25. W. A. Hoffmann, R. M. Marchin, P. Abit, O. Lee Lau, Hydraulic failure and tree dieback are associated with high wood density in a temperate forest under extreme drought. *Glob. Change Biol.* **17**, 2731–2742 (2011).
26. A. Nardini, M. Battistuzzo, T. Savi, Shoot desiccation and hydraulic failure in temperate woody angiosperms during an extreme summer drought. *New Phytol.* **200**, 322–329 (2013).
27. B. Schuldt *et al*., A first assessment of the impact of the extreme 2018 summer drought on central European forests. *Basic Appl. Ecol.* **45**, 86–103 (2020).
28. M. Gharun *et al*., Physiological response of Swiss ecosystems to 2018 drought across plant types and elevation. *Philos. Trans. R. Soc. Lond. B Biol. Sci.* **375**, 20190521 (2020).
29. L. Dietrich, S. Delzon, G. Hoch, A. Kahmen, No role for xylem embolism or carbohydrate shortage in temperate trees during the severe 2015 drought. *J. Ecol.* **107**, 334–349 (2019).
30. H. Hartmann, W. Ziegler, S. Trumbore, Lethal drought leads to reduction in nonstructural carbohydrates in Norway spruce tree roots but not in the canopy. *Funct. Ecol.* **27**, 413–427 (2013).
31. H. Hartmann, W. Ziegler, O. Kolle, S. Trumbore, Thirst beats hunger–Declining hydration during drought prevents carbon starvation in Norway spruce saplings. *New Phytol.* **200**, 340–349 (2013).
32. A. G. Quentin *et al*., Non-structural carbohydrates in woody plants compared among laboratories. *Tree Physiol.* **35**, 1146–1165 (2015).
33. D. P. C. Peters *et al*., Cross-scale interactions, nonlinearities, and forecasting catastrophic events. *Proc. Natl. Acad. Sci. U.S.A.* **101**, 15130–15135 (2004).
34. B. Choat *et al*., Triggers of tree mortality under drought. *Nature* **558**, 531–539 (2018).
35. R. A. Duursma *et al*., On the minimum leaf conductance: Its role in models of plant water use, and ecological and environmental controls. *New Phytol.* **221**, 693–705 (2019).
36. C. Körner, No need for pipes when the well is dry-A comment on hydraulic failure in trees. *Tree Physiol.* **39**, 695–700 (2019).
37. A. Carminati, M. Javaux, Soil rather than xylem vulnerability controls stomatal response to drought. *Trends Plant Sci.* **25**, 868–880 (2020).
38. I. F. Cuneo, T. Knipfer, C. R. Brodersen, A. J. McElrone, Mechanical failure of fine root cortical cells initiates plant hydraulic decline during drought. *Plant Physiol.* **172**, 1669–1678 (2016).
39. C. M. Rodriguez-Dominguez, T. J. Brodribb, Declining root water transport drives stomatal closure in olive under moderate water stress. *New Phytol.* **225**, 126–134 (2020).
40. H. Cochard, A new mechanism for tree mortality due to drought and heatwaves. *bioRxiv* [Preprint] (2019). 10.1101/531632. Accessed 1 October 2020.
41. G. J. Sanders, S. K. Arndt, "Osmotic adjustment under drought conditions" in *Plant Responses to Drought Stress*, R. Aroca, Ed. (Springer, Berlin, Heidelberg, 2012), pp. 199–229.
42. M. T. Tyree, J. S. Sperry, Do woody plants operate near the point of catastrophic xylem dysfunction caused by dynamic water stress?: Answers from a model. *Plant Physiol.* **88**, 574–580 (1988).
43. T. Hölttä, H. Cochard, E. Nikinmaa, M. Mencuccini, Capacitive effect of cavitation in xylem conduits: Results from a dynamic model. *Plant Cell Environ.* **32**, 10–21 (2009).
44. D. D. Breshears *et al*., Tree die-off in response to global change-type drought: Mortality insights from a decade of plant water potential measurements. *Front. Ecol. Environ.* **7**, 185–189 (2009).
45. J.-C. Domec, B. L. Gartner, Cavitation and water storage capacity in bole xylem segments of mature and young Douglas-fir trees. *Trees (Berl.)* **15**, 204–214 (2001).
46. T. J. Brodribb, J. Powers, H. Cochard, B. Choat, Hanging by a thread? Forests and drought. *Science* **368**, 261–266 (2020).
47. MeteoSchweiz, "Hitze und Trockenheit im Sommerhalbjahr 2018–eine klimatologische Übersicht" (Tech. Rep. 272, Fachbericht MeteoSchweiz, Zürich, Switzerland, 2018).
48. K. Ogle, J. J. Barber, C. Willson, B. Thompson, Hierarchical statistical modeling of xylem vulnerability to cavitation. *New Phytol.* **182**, 541–554 (2009).
49. S. M. Landhäusser *et al*., Standardized protocols and procedures can precisely and accurately quantify non-structural carbohydrates. *Tree Physiol.* **38**, 1764–1778 (2018).